Molecular Pharmacology Fast Forward. Published on January 16, 2015 as DOI: 10.1124/mol.114.096222
This article has not been copyedited and formatted. The final version may differ from this version.

MOL #96222

Identification and characterization of a selective allosteric antagonist of human P2X4 receptor channels

Ariel R. Ase, Nicolette S. Honson, Helmi Zaghdane, Tom A. Pfeifer, Philippe Séguéla

Montreal Neurological Institute, Alan Edwards Centre for Research on Pain, Department of Neurology and Neurosurgery, McGill University, Montreal, Canada (A.R.A., P.S.); Screening Division, The Centre for Drug Research and Discovery, Vancouver, Canada (N.S.H., T.A.P.); and Zamboni Chemical Solutions, Department of Chemistry, McGill University, Montreal, Canada (H.Z.)

Molecular Pharmacology Fast Forward. Published on January 16, 2015 as DOI: 10.1124/mol.114.096222
This article has not been copyedited and formatted. The final version may differ from this version.

MOL #96222

Running title: Selective P2X4 antagonist

Address correspondence to:

Philippe Séguéla, Montreal Neurological Institute, 3801 University, Suite 778, Montreal Qc Canada H3A 2B4. E-mail: philippe.seguela@mcgill.ca

Number of text pages: 35

Number of tables: 0

Number of figures: 10

Number of references: 42

Number of words in Abstract: 248

Number of words in Introduction: 655

Number of words in Discussion: 1236

Abbreviations: 5-BDBD, 5-(3-Bromophenyl)-1,3-dihydro-2*H*-benzofuro[3,2-*e*]-1,4-diazepin-2-one; BBG, Brilliant Blue G; PSB-12054, N-(benzyloxycarbonyl)phenoxazine; PSB-12062, N-(p-Methylphenyl)sulfonylphenoxazine; TNP-ATP, 2',3'-*O*-(2,4,6-Trinitrophenyl)adenosine-5'-triphosphate; YO-PRO1, 4-[(Z)-(3-Methyl-1,3-benzoxazol-2(3H)-ylidene)methyl]-1-[3(trimethylammonio)propyl]quinolinium diiodide.

Molecular Pharmacology Fast Forward. Published on January 16, 2015 as DOI: 10.1124/mol.114.096222
This article has not been copyedited and formatted. The final version may differ from this version.

Abstract

P2X4 is an ATP-gated nonselective cation channel highly permeable to calcium. There is increasing evidence that this homomeric purinoceptor expressed in several neuronal and immune cell types is involved in chronic pain and inflammation. The current paucity of unambiguous pharmacological tools available to interrogate or modulate P2X4 function led us to pursue the search for selective antagonists. In the high-throughput screen of a compound library, we identified the phenylurea BX430 (MW= 413) with antagonist properties on human P2X4-mediated calcium uptake. Patch-clamp electrophysiology confirmed direct inhibition of P2X4 currents by extracellular BX430 with submicromolar potency (IC_{50}= 0.54 µM). BX430 is highly selective, having virtually no functional impact on all other P2X subtypes, namely P2X1, P2X2, P2X3, P2X5 and P2X7, at 10 to 100 times its IC_{50}. Unexpected species differences were noticed, as BX430 is a potent antagonist of zebrafish P2X4 but has no effect on rat and mouse P2X4 orthologs. The concentration-response curve for ATP on human P2X4 in presence of BX430 shows insurmountable blockade, indicating a noncompetitive allosteric mechanism of action. Using the YO-PRO1 uptake assay, we observed that BX430 also effectively suppresses ATP-evoked and ivermectin-potentiated membrane permeabilization induced by P2X4 pore dilation. Finally, in single-cell calcium imaging, we validated its selective inhibitory effects on native P2X4 channels at the surface of human THP-1 cells differentiated into macrophages. In summary, this ligand provides a novel molecular probe to assess the specific role of P2X4 in inflammatory and neuropathic conditions, where ATP signaling has been shown to be dysfunctional.

Molecular Pharmacology Fast Forward. Published on January 16, 2015 as DOI: 10.1124/mol.114.096222
This article has not been copyedited and formatted. The final version may differ from this version.

Introduction

The P2X receptor channels are ATP-gated cation channels with high calcium permeability (Jiang et al., 2003; Egan and Khakh, 2004; Khakh and North, 2012). They are formed by assembly of three subunits belonging to a single gene family (P2X1-P2X7), in homomeric or heteromeric channels (Hattori and Gouaux, 2012; Saul et al., 2013). P2X channel subtypes display different sensitivities to ATP, with EC_{50} values ranging from nanomolar to submillimolar concentrations (North, 2002; Coddou et al., 2011). They are expressed in excitable as well as non-excitable cells where they control both membrane potential and intracellular calcium homeostasis, and increasing evidence points to their major involvement in sensory transduction, neuro-immune communication and inflammatory response (Burnstock, 2011).

The homomeric P2X4 channel is widely expressed in central neurons where its role remains to be fully elucidated (Rubio and Soto, 2001; Surprenant and North, 2009). This purinoceptor is also present at the surface of vascular endothelial cells and knockout mice lacking P2X4 have deficits in shear-induced vasodilation, indicating a significant contribution to the regulation of vascular tone (Yamamoto et al., 2006). P2X4 is also expressed in monocytes, macrophages and microglia where it is involved in the release of inflammatory mediators (Bowler et al., 2003; Tsuda et al., 2003; Raouf et al., 2007; Ulmann et al., 2010). It is upregulated at the surface of spinal microglia following peripheral nerve injury and P2X4-mediated brain-derived neurotrophic factor release from microglia has been shown to be a key step in the development of abnormal spinal excitability underlying tactile allodynia in conditions of chronic neuropathic pain (Trang et al, 2012; Tsuda et al., 2012).

Recent reports of the crystal structure of zebrafish P2X4 solved at high resolution in closed as well as ATP-bound open configurations (Kawate et al., 2009, Hattori and Gouaux, 2012)

Molecular Pharmacology Fast Forward. Published on January 16, 2015 as DOI: 10.1124/mol.114.096222
This article has not been copyedited and formatted. The final version may differ from this version.

provided a breakthrough in the understanding of structure-activity relationships that underlie gating mechanisms by specific nucleotides or ion selectivity of P2X receptor channels, however the lack of potent and selective antagonists of P2X4 hinders conclusive investigations of its specific roles using pharmacological approaches *in vitro* and *in vivo*.

Nonselective antagonists for P2X4 include the extensively used nucleotide 2',3'-*O*-(2,4,6-Trinitrophenyl)adenosine-5'-triphosphate (TNP-ATP) with nanomolar potency for P2X1, P2X3 and P2X2+3 subtypes (Lewis et al., 1998; Virginio et al., 1998), the dye Brilliant Blue G (BBG) with higher potency for P2X7 (Jiang et al., 2000), and the monoamine uptake blocker paroxetine with indirect inhibitory effects on the translocation of P2X4 to the cell surface (Nagata et al., 2009). The tricyclic antidepressant amitriptyline modestly inhibits rat and mouse P2X4 at 10 μM and has no effect on human P2X4 (Sim and North, 2010). Recently, N-substituted phenoxazines PSB-12054 (N-(benzyloxycarbonyl)phenoxazine) and PSB-12062 (N-(p-Methylphenyl)sulfonylphenoxazine) were identified as potent and noncompetitive albeit poorly soluble blockers of P2X4 with significant subtype selectivity (Hernandez-Olmos et al., 2012). The same group reported a carbamazepine derivative displaying the properties of a nonselective human P2X4 antagonist that inhibits also P2X1 and P2X3 subtypes (Tian et al., 2014). The benzodiazepine 5-BDBD (5-(3-Bromophenyl)-1,3-dihydro-2*H*-benzofuro[3,2-*e*]-1,4-diazepin-2-one) has been described in a patent as a selective blocker of P2X4 channels with high potency but its full characterization is not reported (Fisher et al., 2005). Competitive inhibitory effects of 5-BDBD on P2X4 appear to be similar in potency to that of TNP-ATP (Casati et al., 2011; Wu et al., 2011; Balázs et al., 2013) while its P2X subtype selectivity remains unknown.

Molecular Pharmacology Fast Forward. Published on January 16, 2015 as DOI: 10.1124/mol.114.096222
This article has not been copyedited and formatted. The final version may differ from this version.

The current paucity of pharmacological tools available to interrogate and modulate P2X4 function led us to pursue the search for small-molecule compounds capable of selectively inhibiting P2X4 receptor channels. We report here the results of a high-throughput screening of a library of chemical compounds using intracellular calcium readout of a stable human P2X4-expressing cell line which allowed us to discover the phenylurea BX430 with allosteric antagonist properties on P2X4 receptor channel activity. Our characterization of this novel potent and subtype-selective P2X4 blocker involves patch-clamp recording, fluorophore uptake assay and single-cell calcium imaging in recombinant preparations as well as in human monocytic THP-1 cells.

Molecular Pharmacology Fast Forward. Published on January 16, 2015 as DOI: 10.1124/mol.114.096222
This article has not been copyedited and formatted. The final version may differ from this version.

Material and Methods

Cell culture

HEK293 cells were cultured in Dulbecco's modified Eagle's medium and 10% heat-inactivated fetal bovine serum (Invitrogen, Carlsbad, CA, USA) containing penicillin and streptomycin. Stable HEK293 cells transfected with human His-tagged P2X4 channels (hP2X4-HEK293 cells) were a kind gift from Dr R. Alan North (University of Manchester). This stable cell line was kept in DMEM:F12 (1:1) containing 10% FBS and 100 units/ml penicillin/streptomycin, supplemented with G-418 (250 µg/ml) for selection. For selectivity studies, HEK293 cells were transiently co-transfected with mCherry and human P2X1, P2X2, P2X3, P2X4, P2X5 or P2X7, or P2X4 of mouse, rat and zebrafish origin in pCDNA3 vector. Transfected cells were used for electrophysiological recordings 48 h to 72 h after transfection.

High-throughput screening

To 384 well plates, 25 µL of extracellular fluid buffer was dispensed using the WellMate (Thermo Scientific). Library compounds were pinned into the buffer using the PlateMate Plus (Matrix Technologies) affixed with the FP3 pin tool to deliver 70 nL of compound to each well. hP2X4-HEK293 cells were loaded with Fluo-2 AM-High Affinity (final concentration 5 µM, Teflabs) and incubated at 37°C, 5% CO_2, on a shaker. After incubating, cells were spun at 1,300 rpm for 4 min to remove excess Fluo-2, and the pellet resuspended in extracellular fluid buffer. Cells were seeded at 10,000 cells/well in 384-well plates using the WellMate. A 10 µL volume of 50% PBS was dispensed to one control column of the plate using the Multidrop Combi 836 liquid dispenser. P2X4-mediated calcium channels were then stimulated by dispensing 10 µL of ATP to remaining wells for a final ATP concentration of 100 µM, and plates were read again for Fluo-2-based intracellular calcium. A total of 26,240 compounds from the

Molecular Pharmacology Fast Forward. Published on January 16, 2015 as DOI: 10.1124/mol.114.096222
This article has not been copyedited and formatted. The final version may differ from this version.

Canadian Chemical Biology Network library were initially screened at 7 µM for inhibition of 100 µM ATP-evoked P2X4-mediated calcium entry. Promising hits from several chemical families were selected for further pharmacological characterization in patch-clamp electrophysiology and single-cell ratiometric calcium imaging. The compound HTS-03052 was purchased from Maybridge for confirmation of 1-(2,6-dibromo-4-isopropyl-phenyl)-3-(3-pyridyl)urea (i.e. BX430) activity.

Ratiometric measurement of intracellular calcium

Stable hP2X4-HEK293 and THP-1 cell lines were loaded with calcium-sensitive fluorescent dye Fura-2 AM (2.5 µM, Molecular Probes) in Ringer's solution containing (in mM): 140 NaCl, 5 KCl, 2 $CaCl_2$, 2 $MgCl_2$, 10 HEPES, and 10 glucose (pH 7.4) with 1% BSA for 30-40 min at 37°C in the dark. Cells were washed two times to remove extracellular Fura-2 AM and left for at least 30 min for complete hydrolysation of acetoxymethyl ester before imaging. Fluorescence measurements of intracellular calcium, in individual cells were performed on an inverted TE2000-U microscope (Nikon) with 40X oil-immersion objective (CFI super(S) fluor, Nikon). Fura-2 was excited alternatively at 340 and 380 nm with a Lambda 10-2 filter wheel (Sutter Instruments) coupled to a xenon arc lamp (XPS-100, Nikon). Fluorescence was monitored at 510 nm and recorded with a high-resolution cooled CCD camera (Cool Snap-HQ, Roper Scientific/Photometrics). Pairs of 340 and 380 nm images were acquired every two second and ratio images were calculated using MetaFluor 7.0 software (Molecular Devices). Intracellular calcium measurement in 96-well black plates was carried out on Victor3^{TM}1420 Multilabel Plate Reader (Perkin Elmer) and ratio of fluorescence intensity measured (fluorescence emission at 510 nm; fluorescence excitation alternating at 340 and 380 nm every 0.5 s). Cells were perfused with Ringer's solution and drugs at room temperature at a flow rate

Molecular Pharmacology Fast Forward. Published on January 16, 2015 as DOI: 10.1124/mol.114.096222
This article has not been copyedited and formatted. The final version may differ from this version.

of 1 ml/min. Results were expressed as the 340/380 nm fluorescent ratio proportional to the intracellular calcium content. The magnitude of responses to ATP was calculated as ΔF/F0, being ΔF= F−F0, and fluorescent background subtracted. Representative current or fluorescent traces were selected to illustrate quantitative data from at least two to three consecutive experiments.

YO-PRO1 Uptake Imaging

ATP-dependent P2X4-mediated pore formation was assessed by imaging the uptake of YO-PRO1 (4-[(Z)-(3-Methyl-1,3-benzoxazol-2(3H)-ylidene)methyl]-1-[3(trimethylammonio)propyl]quinolinium diiodide, Molecular Probes). Stable hP2X4-HEK293 cells were washed with perfusion solution containing (in mM): 140 NaCl, 5 KCl, 2 $CaCl_2$, 2 $MgCl_2$, 10 HEPES, and 10 glucose (pH 7.4), and incubated with 1 μM YO-PRO1 for 30 min. For low-divalent experiments (stated in figure legends as low calcium), cells were washed and placed in low-divalent (0.2 mM $CaCl_2$ and $MgCl_2$-free) perfusion solution containing YO-PRO1 prior to recording. Recordings consisted of a 20-30 min continuous application of ATP. Only healthy cells initially impermeable to YO-PRO1 were selected for recording. Fluorescence changes (excitation, 491 nm; emission, 509 nm) following YO-PRO1 uptake were monitored in individual cells with an inverted TE2000-U microscope (Nikon) equipped with 40X oil-immersion objective and coupled to a xenon arc lamp (XPS-100, Nikon). Images were captured every 10 s on a high-resolution cooled CCD camera (Cool Snap-HQ, Roper Scientific/Photometrics) and processed using MetaFluor 7.0 software (Molecular Devices). Each experiment was repeated at least 3 times.

Electrophysiology

Molecular Pharmacology Fast Forward. Published on January 16, 2015 as DOI: 10.1124/mol.114.096222
This article has not been copyedited and formatted. The final version may differ from this version.

Whole-cell patch-clamp recording of stable hP2X4-HEK293 cells and transiently transfected HEK293 cells (V_{hold}= −60 mV) were performed using pipettes filled with internal solution, pH 7.2, containing (in mM): 120 K-gluconate, 1 $MgCl_2$, 5 EGTA and 10 HEPES. The recording solution, pH 7.4, comprised (in mM): 140 NaCl, 5 KCl, 2 $CaCl_2$, 2 $MgCl_2$, 10 HEPES and 10 glucose. Membrane currents were recorded using an Axopatch 200B amplifier and digitized at 500 Hz with a Digidata 1330 interface (Axon Instruments, Molecular Devices, Sunnyvale, CA, USA). Only recordings with series resistance below 10 MΩ and stable for the duration of the recording were considered for analysis. The liquid junction potential was calculated (Clampex, Axon Instruments) to be 3.7 mV and was not compensated. Drugs were dissolved in recording solution and applied using a SF-77B fast perfusion system (Warner Instruments, Hamden, CT, USA) at a rate of 1 ml/min. All experiments were performed at 22°C. For each individual experiment, current amplitudes or total currents (areas under the current traces) before and after drug treatment were compared and expressed as a percentage.

Statistical Analysis

Current amplitudes or ΔF/F0 fluorescence values recorded during agonist application were measured and their average values ± SEM were calculated for comparative analysis. Data are presented as mean ± SEM unless indicated otherwise, and analyzed using Student's *t* test, two-tailed distribution, paired and non-paired, or one-way ANOVA and two-way ANOVA followed by a Bonferroni's multiple comparisons test. Dose-response data, including IC_{50} or EC_{50} values were analyzed using GraphPad Prism (GraphPad Software Inc., San Diego, CA), by fitting data to the following logistic equations:

Y= Bottom + (Top- Bottom)/(1+10^((LogIC_{50}-X)*HillSlope))

Molecular Pharmacology Fast Forward. Published on January 16, 2015 as DOI: 10.1124/mol.114.096222
This article has not been copyedited and formatted. The final version may differ from this version.

or Y= Bottom + (Top- Bottom)/(1+10^((LogEC_{50}-X)*HillSlope)).

Molecular Pharmacology Fast Forward. Published on January 16, 2015 as DOI: 10.1124/mol.114.096222
This article has not been copyedited and formatted. The final version may differ from this version.

Results

Taking advantage of the high calcium permeability of human P2X4 channels expressed in a stable HEK293 cell line (Young et al., 2008), we defined experimental conditions yielding a robust signal to noise ratio for Fura 2-based fluorescence measurements of intracellular calcium levels rise evoked by ATP. As shown in Fig 1A, ATP-evoked calcium responses were sensitive to TNP-ATP, a non-selective P2X4 antagonist at 50 µM. Due to the expression of endogenous metabotropic ATP receptors, we treated the cells with 1 µM thapsigargin, to deplete intracellular calcium stores and thus evaluate the contribution of non-P2X4 channel-mediated ATP responses. The amplitude of ATP-evoked responses showed only a small decrease following thapsigargin treatment (Fig. 1A), suggesting a minor contribution of Gq-coupled purinoceptors to calcium responses in the hP2X4-HEK293 cell line. Based on this experimental strategy, a high throughput screening (HTS) assay (Z'= 0.59, S/N ratio= 13) was designed to search for small organic compounds endowed with antagonistic properties toward human P2X4. Figure 1B illustrates the frequency distribution of inhibitory and facilitatory effects of the 26,240-compound library from the Canadian Chemical Biology Network (CCBN). A set of 30 candidate antagonists showing > 70% inhibition (a threshold chosen visually based on the distribution of hits) and belonging to 5 distinct chemical families was identified (hit rate= 0.4%). Concentration-response curves were generated to confirm activity using compounds directly from the library plates. Compound 1-(2,6-dibromo-4-isopropyl-phenyl)-3-(3-pyridyl)urea (MW= 413.1, XlogP= 4.23) showed superior potency with an IC_{50} of 0.85 µM (Figure 1C). This compound was purchased commercially and retested in triplicate, yielding a similar IC_{50} of 0.78 µM (Figure 1C).

Molecular Pharmacology Fast Forward. Published on January 16, 2015 as DOI: 10.1124/mol.114.096222
This article has not been copyedited and formatted. The final version may differ from this version.

We selected this potent inhibitor (see structure in Fig. 2A), termed BX430 as an acronym of **B**locker of P2**X4** compound #**3.0,** for further characterization. We first tested it in single-cell calcium imaging with Fura-2 as a ratiometric fluorescence method on the hP2X4-HEK293 cells treated with thapsigargin to deplete intracellular calcium store (Fig. 2B). ATP-evoked intracellular calcium responses from vehicle or thapsigargin were quite similar confirming that contribution of intracellular calcium store sensitive to ATP are negligible in this cellular background. Human P2X4-expressing cells treated with thapsigargin plus BX430 showed a significant reduction of the intracellular calcium rise evoked by ATP (Fig. 2C). To verify if the treatment with 1 µM thapsigargin was sufficient to empty intracellular calcium stores, we challenged the hP2X4-HEK293 cells with the muscarinic agonist carbachol instead of ATP. Under this experimental condition, carbachol-evoked responses were fully suppressed (data not shown). Moreover, no inhibitory effect of BX430 on intracellular calcium response was observed in non-transfected HEK293 cells following ATP application, indicating that endogenous metabotropic ATP receptors, mainly the P2Y2 subtype in this background, are not sensitive to BX430 (data not shown).

The calcium uptake measurements used as the basis of our screening readout, can have limitations, including the detection of indirect artefactual effects of the tested compounds on ATP-sensitive pathways regulating intracellular calcium levels. Therefore we performed patch-clamp recordings in the hP2X4-HEK293 cell line to document a direct antagonistic effect of BX430 on P2X4 receptor channels.

Figure 3A shows human P2X4 current responses following ATP application 2 min apart (vehicle). The compound BX430 was then initially tested at 5 µM concentration in pre- and co-application with the agonist ATP. BX430 potently inhibited ATP-evoked current responses and

Molecular Pharmacology Fast Forward. Published on January 16, 2015 as DOI: 10.1124/mol.114.096222
This article has not been copyedited and formatted. The final version may differ from this version.

P2X4 currents showed a complete recovery to baseline values after a washout period, indicating a reversible blockade (see also quantitative results in right panel of Fig 3A). For comparison, we tested under the same experimental conditions the competitive antagonist 5-BDBD (Fisher et al., 2005; Balázs et al., 2013). Although 5-BDBD (10 μM) showed a slight decrease in the current amplitude evoked by ATP in the stable hP2X4-HEK293 cell line, the effect was not found significant (Fig 3B; $p= 0.218$; $n= 4-5$). Therefore, BX430 is definitely more potent than 5-BDBD under the same experimental conditions (current amplitude in control= 90%; $p < 0.05$; $n= 8$ vs. current amplitude with BX430= 10%; $p < 0.001$; $n= 8$).

We next assessed the potency (IC_{50}) of BX430 on the P2X4-mediated ATP-evoked currents in patch clamp recordings in hP2X4-HEK293 cells. The sigmoidal BX430 dose-response curves for inhibition of maximal current amplitude and total current were fitted to the logistic equation, giving an $IC_{50}= 0.55$ μM with a slope nH= -1.00 and an $IC_{50}= 0.54$ μM with a slope nH= -0.86, respectively (Fig. 4A and B). The compound BX430 binds to a single site and the binding follows the law of mass action as the time constant of P2X4 current decay is linearly related to its concentration with an association rate= 0.96 $\mu M^{-1}.ms^{-1}$ and a dissociation rate= 0.53 ms^{-1} ($R^2= 0.95$, data not shown).

To further characterize the antagonist effect of BX430 on the P2X4 receptor channel response, we asked if the compound exerts its effect extracellularly or intracellularly, i.e. on intracellular domains of the P2X4 channel or some intracellular components important for P2X4 function. BX430 (5 μM) was found to significantly reduce both peak (about –29%) and total current (about –75%) of P2X4 channel response when co-applied with ATP without pre-incubation (Fig. 5A), strongly suggesting that the antagonist acts on the receptor channel from the extracellular space, by binding either on the ectodomain or on the transmembrane domains.

Molecular Pharmacology Fast Forward. Published on January 16, 2015 as DOI: 10.1124/mol.114.096222
This article has not been copyedited and formatted. The final version may differ from this version.

We also recorded P2X4 currents with BX430 applied intracellularly through the patch pipette. No major effect on P2X4 current amplitude or kinetics was observed when the pipette solution reached the equilibrium with the intracellular milieu, as shown by the consecutive ATP-evoked current responses as shown (Fig. 5B). The size of the initial ATP responses was identical to that recorded in cells with control intracellular solution without BX430 (Fig. 5A and B). Moreover, application of extracellular BX430 (5 µM) during the desensitizing phase of the P2X4 current evoked an "immediate" acceleration of the relaxation (Fig. 5C). The inhibitory effect of 1 µM BX430 was not sensitive to increasingly hyperpolarizing membrane potentials, from –20 mV (49 ± 2% blockade, n= 4) to –80 mV (52 ± 2 % blockade, n= 6) (data not shown). These results indicate that the compound BX430, uncharged at physiological pH, does not sense membrane voltage and is not a direct pore channel blocker.

In order to investigate whether the inhibition of P2X4 activity is competitive or non-competitive, electrophysiological recordings were performed in hP2X4-HEK293 cells at different concentrations of ATP with a fixed concentration of antagonist (1 µM). Concentration-response curves in the absence and presence of BX430, in which current amplitude was normalized to the current activated by the highest concentration of ATP (1 mM), gave an EC_{50} value of 7.3 µM with a slope nH of 0.99 in the absence of BX430, and an EC_{50} of 187 µM with a slope nH of 0.49 in the presence of 1 µM BX430 (Fig. 6). The inhibitory effect of BX430 could not be overcome with increasing concentrations of ATP up to 1 mM. These two effects, i.e. a shift in ATP EC_{50} and a reduction in maximal response at saturating concentrations of ATP, indicate that BX430 is a non-competitive antagonist binding to an allosteric site on the P2X4 receptor channel.

Molecular Pharmacology Fast Forward. Published on January 16, 2015 as DOI: 10.1124/mol.114.096222
This article has not been copyedited and formatted. The final version may differ from this version.

The human P2X channel family is composed of six homomeric functional subtypes. We tested potential effects of BX430 on current amplitude, kinetics and recovery of the subtypes P2X1, P2X2, P2X3, P2X4, P2X5 and P2X7 in transiently transfected HEK293 cells. We observed a high degree of selectivity of BX430 toward P2X4, as no difference in current amplitude or phenotype was detected on all other human P2X channel subtypes when used at 10 times its IC_{50} for human P2X4 (Fig. 7). We confirmed in these experiments that BX430 showed similar potency between wild-type human P2X4 in transiently transfected HEK293 cells and the His-tagged version used for HTS in the stable HEK293 cell line. As P2X4 and P2X7 are natively co-expressed in many cell types, a potential inhibition of human P2X7 by 50 µM BX430 (around 100 times its IC_{50} for human P2X4) was also tested, without any significant effect (data not shown).

The primary sequence of P2X4 subunits is significantly conserved between vertebrates from fish to primates, therefore we investigated the sensitivity of several P2X4 channel orthologs to BX430. Unexpectedly, mouse P2X4 (87% amino acid identity with human P2X4) in transiently transfected HEK293 cells did not show any inhibition when BX430 was applied at 10 µM (Fig. 8A,B), a concentration that produces a strong blockade of human P2X4 (Fig. 6). BX430 did not have any significant effect on the rat P2X4 either (87% and 94% amino acid identity with human and mouse P2X4, respectively), under the same experimental conditions (data not shown). However we observed that zebrafish P2X4, despite a weaker sequence homology (57% amino acid identity with human P2X4), is effectively blocked by BX430 (Fig. 8B,C) with an IC50= 1.89 µM (data not shown).

Ivermectin, an anti-parasitic agent extensively used in human and veterinary medicine, is also used as a pharmacological tool in basic research as a potent positive allosteric modulator to

Molecular Pharmacology Fast Forward. Published on January 16, 2015 as DOI: 10.1124/mol.114.096222
This article has not been copyedited and formatted. The final version may differ from this version.

pharmacologically identify P2X4 receptor channels in native preparations (Khakh et al., 1999; Burkhart, 2000; Priel and Silberberg, 2004). Using patch-clamp recording, we confirmed that 3 μM ivermectin potentiates 50 μM ATP-evoked human P2X4 currents (Fig. 9). Treatment with 10 μM BX430 significantly inhibited ivermectin-potentiated P2X4 current response (67%) as shown quantitatively in Fig 9A. A typical biophysical property of several slowly-desensitizing P2X channel subtypes, including P2X4, is their ability to generate a large pore that allows the passage of molecules up to 900 Da under continuous stimulation with ATP (Khakh and Lester, 1999, Bernier et al. 2012). We took advantage of a robust fluorescence assay based on ATP-evoked YO-PRO 1 uptake to test whether BX430 has an inhibitory effect on dilation of the P2X4 pore, in the presence of ivermectin to facilitate pore dilation in normal extracellular divalents. In line with our previous results, we observed that P2X4-mediated YO-PRO 1 uptake was significantly blocked by 5 μM BX430 (Fig. 9B).

Lastly we tested the inhibitory effects of BX430 on native P2X4 receptor channels expressed in the THP-1 cells, a human monocytic cell line that can be differentiated in macrophages with the phorbol ester 12-O-tetradecanoylphorbol-13-acetate. As depicted in Fig. 10, ATP applied at 50 μM to prevent activation of P2X7 (EC_{50}= 300 μM), was able to evoke robust intracellular calcium responses in phorbol ester-differentiated THP-1 cells. When the cells were exposed to BX430 (5 μM), the amplitude of ATP-evoked intracellular calcium responses was markedly reduced (quantitative data in Fig. 10B). We recorded calcium responses evoked by 100 μM BzATP, a more potent P2X7 agonist (EC_{50}= 30 μM), confirming the co-expression of P2X7 in differentiated THP-1 cells. Treatment with the selective P2X7 antagonist Brilliant Blue (BBG, 1 μM) was without any effect on 50 μM ATP-evoked calcium responses (Fig. 10C) but significantly blocked BzATP-evoked P2X7-mediated calcium responses (Fig. 10D). This

Molecular Pharmacology Fast Forward. Published on January 16, 2015 as DOI: 10.1124/mol.114.096222
This article has not been copyedited and formatted. The final version may differ from this version.

indicated that 50 µM ATP was selectively activating BX430-sensitive P2X4 receptor channels without evoking significant BBG-sensitive BX430-insensitive P2X7-mediated calcium responses in THP-1 cells.

Molecular Pharmacology Fast Forward. Published on January 16, 2015 as DOI: 10.1124/mol.114.096222
This article has not been copyedited and formatted. The final version may differ from this version.

Discussion

High-throughput screening of a library of compounds using ATP-evoked calcium uptake assay in a stable hP2X4-HEK293 cell line allowed us to identify BX430, a phenylurea endowed with potent (IC_{50}= 0.555 µM) and selective antagonist properties on recombinant as well as native human P2X4 receptor channels.

Confirming the high calcium permeability of human P2X4 channels reflected by a fractional current Pf close to 15% (Egan and Khakh, 2004), ATP-evoked calcium responses were robust and reproducible, with only a minor contribution by endogenous P2Y receptors in this hP2X4-HEK293 cell line. Therefore the sensitive screening method described here has the potential to identify novel lead compounds that block P2X4 receptor channels. Moreover, with simple adjustments of the recording parameters, such a calcium-based cellular assay can also be used to screen for positive allosteric modulators of P2X4 function (see Fig. 1B). The blocker BX430, selected among other inhibitory lead compounds in the CCBN library for its potency and selectivity for P2X4, was found to be highly soluble in physiological solutions and stable at room temperature, and it showed the same inhibitory effects during several hours of recording.

Several non-specific P2X4 antagonists have been reported previously (Nagata et al., 2009; North and Jarvis, 2013), including TNP-ATP (IC_{50}= 15.2 µM) and paroxetine (IC_{50}= 1.87 µM). Recently, the phenoxazines PSB-12054 (IC_{50}= 0.19 µM) and PSB-12062 (IC_{50}= 0.93 µM) have been described as relatively selective blockers of P2X4-mediated calcium responses but they were not tested on P2X4-mediated currents (Hernandez-Olmos et al., 2012). These phenoxazines possess low water solubility hindering their use in many experimental conditions. Another compound with reported inhibitory properties against P2X4 receptor channels is the benzodiazepine 5-BDBD, which was reported to block P2X4 currents in

Molecular Pharmacology Fast Forward. Published on January 16, 2015 as DOI: 10.1124/mol.114.096222
This article has not been copyedited and formatted. The final version may differ from this version.

recombinant preparations with an IC_{50}= 0.5 μM (Fisher at al., 2005). Unfortunately, the results were described in a corporate patent and details of the experimental procedures are not available. Balázs and collaborators (2013), using both calcium imaging and patch-clamp electrophysiology, reported that 5-BDBD is a somewhat potent (IC_{50}= 1.6 μM) but competitive antagonist against human P2X4 in HEK293 cells when it is activated by 0.25-1 μM ATP. In our hands, 5-BDBD, tested at 10 μM on human P2X4 responses evoked by 50 μM ATP, shows a minor effect with less than 20% decrease in the currents. These striking differences in efficacy of 5-BDBD demonstrate the advantage of non-competitive ligands like BX430 which inhibitory effects on P2X4 responses do not depend on ATP levels.

Even when co-applied with ATP without pre-incubation, BX430 showed a remarkable effect on the phenotype of human P2X4 current. This fact and the observation that BX430 does not induce any inhibition when it is applied intracellularly suggest that BX430 acts from the extracellular side of the plasma membrane. The dose-response curve of ATP on human P2X4, with and without BX430, showed an insurmountable blockade up to 1 mM ATP, clearly indicating a noncompetitive mechanism of action. Also, knowing that the efficacy of BX430 is not voltage-dependent, we can discard the possibility that BX430 acts as a channel blocker by plugging the cationic pore of P2X4. Therefore we conclude from these data that the most likely mechanism of action of BX430 on P2X4 receptor channel activity is a change of subunit conformation triggered by its binding to an allosteric site located on the ectodomain or the transmembrane domains with access from the extracellular space.

To test the potential involvement of P2X4 in any physiological process using pharmacology, a highly selective tool is needed. The ligand BX430 seems to be remarkably selective for P2X4, as no effect (inhibitory or facilitatory) was observed on currents mediated by the human P2X1,

Molecular Pharmacology Fast Forward. Published on January 16, 2015 as DOI: 10.1124/mol.114.096222
This article has not been copyedited and formatted. The final version may differ from this version.

P2X2, P2X3, P2X5, P2X7 subtypes when tested at ten times its IC_{50} for P2X4, either on peak amplitude, total current or recovery time. As the P2X7 and P2X4 purinoceptors are known to be co-expressed in many non-neuronal cell types including monocytes, macrophages, microglia and airway ciliated cells (Bowler et al., 2003; Xiang and Burnstock, 2005; Ma et al., 2006; Guo et al., 2007), BX430 was re-tested on human P2X7 at about hundred times its IC_{50} for P2X4, without showing any effect.

Regarding the sensitivity of P2X4 from other species to BX430, we noticed that this compound effectively inhibited zebrafish P2X4 while it had little or no effect on rodent P2X4 current responses. Several members of the P2X family, including P2X4 and P2X7, have been reported to show large species differences in antagonistic potencies between human and rodent receptors (North and Surprenant, 2000; Gever et al., 2006; Buell et al., 1996; Jones et al., 2000; Michel et al., 2009). Indeed Hernandez-Olmos and collaborators (2012) recently observed that the compound PSB-12054 was much more potent on human P2X4 than on rodent P2X4 orthologs. From a structural point of view, it will be interesting to analyze sequences and protein alignments between a number of P2X4 orthologs sensitive and insensitive to BX430 as a potential strategy to identify the aminoacids/domains responsible for the effects of this novel antagonist.

Ivermectin, a positive allosteric regulator of P2X4 channels, strongly increased ATP-evoked human P2X4 currents as previously reported (Khakh et al., 1999; Priel and Silberberg, 2004) and its potentiating effect was suppressed by BX430. Prolonged stimulation of P2X4 with ATP, facilitated by ivermectin, causes the ion channel to dilate, leading to the formation of a pore that is permeable to large molecules (Bernier et al., 2012; Rokic and Stojilkovic, 2013).

Molecular Pharmacology Fast Forward. Published on January 16, 2015 as DOI: 10.1124/mol.114.096222
This article has not been copyedited and formatted. The final version may differ from this version.

Interestingly, in presence of BX430, ATP-evoked P2X4 pore dilation was almost completely abolished. To our knowledge, this is the first time that a P2X4 antagonist is used to inhibit pore dilation.

Tsuchiya and collaborators (1980) established the human THP-1 cell line, which became increasingly used as a source of primary monocytes and macrophages. After exposure to phorbol esters, THP-1 cells, initially rounded and in suspension, start to adhere to culture plates accompanied by differentiation into a macrophage phenotype, with marked morphological changes in cell shape and organelles (Auwerx, 1991; Park et al., 2007). Signaling via extracellular ATP alters the outcome of inflammation by mounting appropriate macrophage responses against foreign agents or tumors, or conversely, by promoting chronic inflammation during ischemia or chronic pain (Idzko et al., 2014). It has been reported that human macrophages expressed several ATP-sensitive P2 receptors including P2X1, P2X4, P2X7 and P2Y2. In our experiments, ATP-evoked calcium responses in differentiated THP-1 cells were very sensitive to BX430. Therefore, based on the absence of any effect of BX430 on P2X1 and P2X7 currents or on P2Y2-mediated calcium responses, we confirmed the expression of functional P2X4 receptors at the surface of THP-1-derived macrophages (Li and Fountain, 2012).

Guo et al. (2007) provided convincing evidence for the existence of functional P2X4+7 heteromeric channels sensitive to the antagonist BBG. The absence of inhibitory effect of BBG on ATP-evoked calcium responses strongly suggests that the population of P2X4+7 heteromers, if present, is a minor component in differentiated THP-1 cells. This is in agreement with several studies in which co-expressed homomeric P2X4 and homomeric P2X7 receptor

Molecular Pharmacology Fast Forward. Published on January 16, 2015 as DOI: 10.1124/mol.114.096222
This article has not been copyedited and formatted. The final version may differ from this version.

channels have been shown to constitute the main P2X populations in immune cells (Boumechache et al., 2009) as well as in heterologous expression systems (Antonio et al., 2011).

In summary, our study describes the identification of the phenylurea BX430 with high potency and selectivity for P2X4 receptor channels. This ligand will provide a novel pharmacological tool to specifically investigate the role of human P2X4 in physiological and pathological conditions where ATP signaling has been shown to be dysfunctional, including inflammatory diseases.

Molecular Pharmacology Fast Forward. Published on January 16, 2015 as DOI: 10.1124/mol.114.096222
This article has not been copyedited and formatted. The final version may differ from this version.

Acknowledgments: The authors thank Van Nguyen (McGill University) for her technical help with cell culture and transfection.

Authorship Contribution:

Participated in research design: Ase, Honson, Pfeifer, Séguéla.

Conducted experiments: Ase, Honson, Zaghdane.

Contributed new reagents or analytic tools: Zaghdane.

Performed data analysis: Ase, Honson, Pfeifer, Séguéla.

Wrote or contributed to the writing of the manuscript: Ase, Honson, Pfeifer, Séguéla.

References

Antonio LS, Stewart AP, Xu XJ, Varanda WA, Murrell-Lagnado RD, and Edwarson JM (2011) P2X4 receptors interact with both P2X2 and P2X7 receptors in the form of homotrimers. *Br J Pharmacol* **163**:1069-1077.

Auwerx J (1991) The human leukemia cell line, THP-1: a multifacetted model for the study of monocyte-macrophage differentiation. *Experientia* **47**:22-31.

Balázs B, Dankó T, Kovács G, Köles L, Hediger MA and Zsembery A (2013) Investigation of the inhibitory effects of the benzodiazepine derivative, 5-BDBD on P2X4 purinergic receptors by two complementary methods. *Cell Physiol Biochem* **32**:11-24.

Bernier LP, Ase AR, Boué-Grabot E, and Séguéla P (2012) P2X4 receptor channels form large noncytolytic pores in resting and activated microglia. *Glia* **60**:728-37.

Boumechache M, Masin M, Edwardson JM, Gorecki DC, and Murrell-Lagnado R (2009) Analysis of assembly and trafficking of native P2X4 and P2X7 receptor complexes in rodent immune cells. *J Biol Chem* **284**:13446–13454.

Bowler JW, Bailey RJ, North RA, and Surprenant A (2003) P2X4, P2Y1 and P2Y2 receptors on rat alveolar macrophages. *Br J Pharmacol* **140**:567-575.

Buell G, Collo G, and Rassendren F (1996) P2X receptors: an emerging channel family. *Eur J Neurosci* **8**:2221-8.

Burkhart, CN (2000) Ivermectin: an assessment of its pharmacology, microbiology and safety. *Vet Hum Toxicol* **42**:30-35.

Burnstock G (2011) Introductory overview of purinergic signalling. *Front Biosci* **3**:896-900.

Casati A, Frascoli M, Traggiai E, Proietti M, Schenk U, and Grassi F (2011) Cell-autonomous regulation of hematopoietic stem cell cycling activity by ATP. *Cell Death Differ* **18**:396-404.

Coddou C, Yan Z, Obsil T, Huidobro-Toro JP, and Stojilkovic SS (2011) Activation and regulation of purinergic P2X receptor channels. *Pharm Rev* **63**:641-683.

Egan TM and Khakh BS (2004) Contribution of calcium ions to P2X channel responses. *J Neurosci* **24**:3413-3420.

Fisher R, Grützmann R, Blasco HPJ, Kalthof B, Gadea PC, Stelte-Ludwig B, Woltering E and Wutke M (2005) Benzofuro-1,4-diazepin-2-one derivatives. Patent number: EP1608659A1, 1-14.

Gever JR, Cockayne DA, Dillon MP, Burnstock G and Ford AP (2006) Pharmacology of P2X channels. *Pflugers Arch* **452**:513-537.

Guo C, Masin M, Qureshi OS and Murrell-Lagnado RD (2007) Evidence for functional P2X4/P2X7 heteromeric receptors. *Mol Pharmacol* **72**:1447-1456.

Hattori M and Gouaux E (2012) Molecular mechanism of ATP binding and ion channel activation I P2X receptors. *Nature* **485**:207-212.

Hernandez-Olmos V, Abdelrahman A, El-Tayeb A, Freudendahl D, Weinhausen S, and Müller CE (2012) N-substituted phenoxazine and acridone derivatives: structure-activity relationships of potent P2X4 receptor antagonists. *J Med Chem* **55**:9576-9588.

Jiang LH, Mackenzie AB, North RA, and Surprenant A (2000) Brilliant blue G selectively blocks ATP-gated rat P2X(7) receptors. *Mol Pharmacol* **58**:82-88.

Jiang LH, Kim M, Spelta V, Bo X, Surprenant A and North RA (2003) Subunit arrangement in P2X receptors. *J Neurosci* **23**:8903-8910.

Jones CA, Chessell IP, Simon J, Barnard EA, Miller KJ, Michel AD, and Humphrey PP (2000) Functional characterization of the P2X(4) receptor orthologues. *Br J Pharmacol* **129**:388-94.

Idzco M, Ferrari D, and Eltzschig HK (2014) Nucleotide signaling during inflammation. *Nature* **509**:310-317.

Kawate T, Michel JC, Birdsong WT and Gouaux E (2009) Crystal structure of the ATP-gated P2X(4) ion channel in the closed state. *Nature* **460**:592-598.

Khakh BS and North RA (2012) Neuromodulation by extracellular ATP and P2X receptors in the CNS. *Nature* **76**:51-60.

Khakh BS and Lester HA (1999) Dynamic selectivity filters in ion channels. *Nature* **23**:653-658.

Khakh BS, WR Proctor TV Dunwiddie C Labarca and Lester HA (1999) Allosteric control of gating and kinetics at $P2X_4$ receptor channels. *J Neurosci* **19**:7289-7299.

Lewis CJ, Surprenant A, and Evans RJ (1998) 2',3'-O-(2,4,6- trinitrophenyl) adenosine 5'-triphosphate (TNP-ATP)-a nanomolar affinity antagonist at rat mesenteric artery P2X receptor ion channels. *Br J Pharmacol* **124**:1463-6.

Li J and Fountain SJ (2012) Fluvastatin suppresses native and recombinant human P2X4 receptor function. *Purinergic Signal* **8**:311-6.

Ma W, Korngreen A, Weil S, Cohen EB, Priel A, Kuzin L and Silberberg SD (2006) Pore properties and pharmacological features of the P2X receptor channel in airway ciliated cells. *J Physiol* **571**:503-517.

Michel AD, Ng SW, Roman S, Clay WC, Dean DK, and Walter DS (2009) Mechanism of action of species-selective P2X(7) receptor antagonists. *Br J Pharmacol* **156**:1312-1325.

Nagata K, Imai T, Yamashita T, Tsuda M, Tozaki-Saitoh H, and Inoue K (2009) Antidepressants inhibit P2X4 receptor function: a possible involvement in neuropathic pain relief. *Mol Pain* **23**:20.

North RA and Jarvis MF (2013) P2X receptors as drug targets. *Mol Pharmacol* **83:**759-769.

North RA (2002) Molecular physiology of P2X receptors *Physiol Rev* **82**:1013-1067.

North RA and Surprenant A (2000) Pharmacology of cloned P2X receptors. *Annu Rev Pharmacol Toxicol* **40**:563-580.

Park EK1, Jung HS, Yang HI, Yoo MC, Kim C, and Kim KS (2007) Optimized THP-1 differentiation is required for the detection of responses to weak stimuli. *Inflamm Res* **56**:45-50.

Priel A and Silberberg SD (2004) Mechanism of ivermectin facilitation of human P2X4 receptor channels *JGP* **123**:281-293.

Raouf R, Chabot-Doré AJ, Ase AR, Blais D, and Séguéla P (2007) Differential regulation of microglial P2X4 and P2X7 ATP receptors following LPS-induced activation. *Neuropharmacology* **53**:496-504.

Rokic MB and Stojilkovic SS (2013) Two open states of P2X receptor channels. *Front Cell Neurosci* **14**:215.

Rubio ME and Soto F (2001) Distinct localization of P2X receptors at excitatory postsynaptic specializations. *J Neurosci* **21:**641-653.

Saul A, Hausmann R, Kless A, and Nicke A (2013) Heteromeric assembly of P2X subunits. *Front Cell Neurosci* **18**:250.

Sim JA and North RA (2010) Amitriptyline does not block the action of ATP at human P2X4 receptor. *Br J Pharmacol* **160**:88-92.

Surprenant A and North RA (2009) Signaling at purinergic P2X receptors. *Annu Rev Physiol* **71**:333-359.

Tian M, Abdelrahman A, Weinhausen S, Hinz S, Weyer S, Dosa S, El-Tayeb A, and Müller CE (2014) Carbamazepine derivatives with P2X4 receptor-blocking activity. *Bioorg Med Chem* **22**:1077-1088.

Trang T, Beggs S, and Salter MW (2012) ATP receptors gate microglia signaling in neuropathic pain. *Exp Neurol* **234**:354-361.

Tsuchiya S, Yamabe M, Yamaguchi Y, Kobayashi Y, Konno T, and Tada K (1980) Establishment and characterization of a human acute monocytic leukemia cell line (THP-1). *Int J Cancer* **26**:171-6.

Tsuda M, Shigemoto-Mogami Y, Koisumi S, Mizokoshi A, Kohsaka S, Salter MW, and Inoue K (2003) P2X4 receptors induced in spinal microglia gate tactile allodynia after nerve injury. *Nature* **424**:778-783.

Tsuda M, Tozaki-Saitoh H, and Inoue K (2012) Purinergic system, microglia and neuropathic pain. *Curr Opin Pharmacol* **12**:74-79.

Ulmann L, Hirbec H, and Rassendren F (2010) P2X4 receptors mediate PGE2 release by tissue-resident macrophages and initiate inflammatory pain. *EMBO J* **29**:2290-300.

Virginio C, Robertson G, Surprenant A, and North RA (1998) Trinitrophenyl-substituted nucleotides are potent antagonists selective for P2X1, P2X3, and heteromeric P2X2/3 receptors. *Mol Pharmacol* **53**:969-73.

Wu T, Dai M, Shi XR, Jiang ZG, and Nuttall AL (2011) Functional expression of P2X4 receptor in capillary endothelial cells of the cochlear spiral ligament and its role in regulating the capillary diameter. *Am J Physiol Heart Circ Physiol* **301**:H69-78.

Xiang Z and Burnstock G (2005) Expression of P2X receptors on rat microglial cells during early development. *Glia* **52**:119-126.

Yamamoto K, Sokabe T, Matsumoto T, Yoshimura K, Shibata M, Ohura N, Fukuda T, Sato T, Sekine K, Kato S, Isshiki M, Fujita T, Kobayashi M, Kawamura K, Masuda H, Kamiya A, and Ando J (2006) Impaired flow-dependent control of vascular tone and remodeling in P2X4-deficient mice. *Nature Med* **12**:133-7.

Young MT, Fisher JA, Fountain SJ, Ford RC, North RA, and Khakh BS (2008) Molecular shape, architecture, and size of P2X4 receptors determined using fluorescence resonance energy transfer and electron microscopy. *J Biol Chem* **283**:26241-51.

Molecular Pharmacology Fast Forward. Published on January 16, 2015 as DOI: 10.1124/mol.114.096222
This article has not been copyedited and formatted. The final version may differ from this version.

Footnote

This work was supported by grants from the Canadian Institutes of Health Research [MOP-130239] and the Natural Sciences and Engineering Council of Canada [DG-203061], with the contribution of the Centre for Drug Research and Discovery. The authors have no conflicting financial interests.

Molecular Pharmacology Fast Forward. Published on January 16, 2015 as DOI: 10.1124/mol.114.096222
This article has not been copyedited and formatted. The final version may differ from this version.

Figure Legends

Figure 1. Validation of the stable hP2X4-HEK293 cell line for HTS and identification of a candidate P2X4 antagonist.

(A) Robust ATP-evoked calcium responses measured in hP2X4-HEK293 cells were sensitive to high concentrations of the non-selective P2X4 antagonist TNP-ATP (50 µM). Treatment with thapsigargin (Thap, 1 µM), to deplete intracellular calcium stores, induced a small decrease in ATP response, suggesting a minor contribution of endogenous metabotropic ATP receptors. *P*< 0.0001 (n= 6) between thapsigargin and thapsigargin + TNP-ATP-treated cells. **(B)** Distribution of ATP-evoked intracellular calcium responses in HTS showing inhibitory and facilitory effects of the 26,240 compounds from the CCBN library tested on the hP2X4-HEK293 cell line. The dashed red line indicates the 70% inhibition criteria used to identify actives from the screen. **(C)** Concentration-response curves of BX430 obtained directly from the CCBN screening library (n= 1, represented by empty squares and a dashed line, IC_{50}= 0.85 µM) or from a commercial source (n= 3, represented by filled circles and a solid line, IC_{50}= 0.78 µM).

Figure 2. Structure of BX430 and blockade of ATP-evoked calcium responses.

(A) Structure of the phenylurea BX430. **(B)** ATP (50 µM) evokes robust intracellular calcium responses in the stable hP2X4-HEK293 cell line, in the absence or presence of thapsigargin (1 µM). But when cells were exposed to BX430, intracellular calcium response showed a marked reduction. (**C**) Quantitative results are shown on the right panel. ***P< 0.001; ****P< 0.0001 (n= 14-30) versus vehicle treated cells.

Molecular Pharmacology Fast Forward. Published on January 16, 2015 as DOI: 10.1124/mol.114.096222
This article has not been copyedited and formatted. The final version may differ from this version.

Figure 3. The ligand BX430 is a direct P2X4 antagonist.

(A) P2X4 current responses evoked by ATP applications 2 min apart in the stable hP2X4-HEK293 cell line. BX430 (5 μM), co-applied with the agonist ATP (50 μM) after 2 min pre-incubation blocked significantly ATP-evoked currents. Recovery after washout indicates that the inhibitory effect of BX430 is reversible. **(B)** Comparison with the inhibitory effect of the antagonist 5-BDBD under the same experimental conditions. ****P*< 0.001 (n= 9-12)

Figure 4. Submicromolar potency of BX430 on human P2X4 receptor channels.

The normalized dose-response curves were established in patch clamp electrophysiology using the stable hP2X4-HEK293 cell line with 50 μM ATP, and fitted with a logistic equation giving an IC_{50}= 0.55 μM and an IC_{50}= 0.54 μM for maximal (peak) current (A) and total current (B), respectively (n= 9-12).

Figure 5. BX430 acts on P2X4 channels from the extracellular side.

(A) BX430 (5 μM) showed pronounced inhibitory effect on P2X4 channel currents in hP2X4-HEK293 cells when co-applied with ATP extracellularly without pre-incubation. The quantitative results on peak vs. total current reflect the effect of BX430 blockade on desensitization kinetics. ***P*< 0.01; ****P*< 0.001 (n= 5-6) versus vehicle treated cells. **(B)** When BX430 (5 μM) is applied intracellularly via the patch pipette, no change in current amplitude was observed when the pipette solution is expected to have reached equilibrium with the intracellular milieu (4 min). **(C)** Fast antagonist effect of extracellular BX430 (5 μM) on ATP-evoked P2X4 current when applied during the phase of desensitization, in representative control (1), test (2) and washout (3) conditions.

Molecular Pharmacology Fast Forward. Published on January 16, 2015 as DOI: 10.1124/mol.114.096222
This article has not been copyedited and formatted. The final version may differ from this version.

Figure 6. BX430 is a non-competitive allosteric P2X4 antagonist.

Concentration-response relationships obtained in stably transfected hP2X4-HEK293 cells, in the absence (vehicle) and presence of BX430 (0.5-1 µM), with P2X4 current normalized to the current activated by 1 mM ATP in control condition. Concentration-response curves are fitted with an ATP EC_{50}= 7.3 µM and a slope nH= 0.99 in the absence of BX430, compared to an ATP EC_{50}= 187.3 µM and a slope nH= 0.49 in the presence of BX430. The inhibitory effect of BX430 cannot be overcome with increasing ATP concentrations up to 1 mM (n= 4-7).

Figure 7. BX430 shows a high degree of selectivity toward the P2X4 subtype.

P2X subtype selectivity of BX430 was tested at 5 µM (around 10 times the IC_{50} for human P2X4) in transiently transfected HEK293 cells. Typical recordings of ATP-evoked currents mediated by human receptor channels P2X1, P2X2, P2X3, P2X4, P2X5 and P2X7 in presence or absence of BX430 are shown, along with quantitative results. *P< 0.05 (n= 4-6).

Figure 8. Sensitivity of P2X4 to BX430 is species-dependent.

(A, B) Mouse P2X4 receptor channels in transiently transfected HEK293 cells are insensitive to treatment with 10 µM BX430 while ATP-evoked zebrafish P2X4-mediated responses are significantly inhibited **(C,D)**. *P< 0.05; **P< 0.01 (n= 4-7) versus vehicle treated cells.

Figure 9. Blockade of ivermectin potentiation and P2X4 large pore formation by BX430.

(A) Using patch-clamp recording, we observed strong inhibitory effects of BX430 on P2X4 currents potentiated by ivermectin (IVM, 3 µM) as illustrated here by the quantitative results. White bars 1 and 3 correspond to normalized control ATP-evoked currents before ivermectin and after washout, respectively. Black bars 4 and 6 correspond to normalized control ATP-

Molecular Pharmacology Fast Forward. Published on January 16, 2015 as DOI: 10.1124/mol.114.096222
This article has not been copyedited and formatted. The final version may differ from this version.

evoked currents before ivermectin + BX430 (5 µM) and after washout, respectively. *P< 0.05; ***P< 0.001 (n= 4). **(B)** ATP-evoked YO-PRO 1 entry reflecting P2X4 pore formation in the hP2X4-HEK293 cell line in presence of ivermectin (IVM) and significant blockade by BX430 (5 µM) (n= 16-25). ****P< 0.0001 (n= 16-25).

Figure 10. BX430-sensitive human P2X4 receptor channels are expressed at the surface of differentiated THP-1 cells.

(A) ATP (50 µM) evokes robust BX430-sensitive intracellular calcium responses in THP-1 cells. **(B)** Quantitative results. **(C)** P2X7 (EC50= 300 µM) does not contribute significantly to the intracellular calcium responses evoked by the application of 50 µM ATP as they are insensitive to the P2X7 antagonist BBG (1 µM), in contrast to BzATP-evoked intracellular calcium responses **(D)**. *P< 0.05; ***P< 0.001 (n= 11-42).

Figure 1

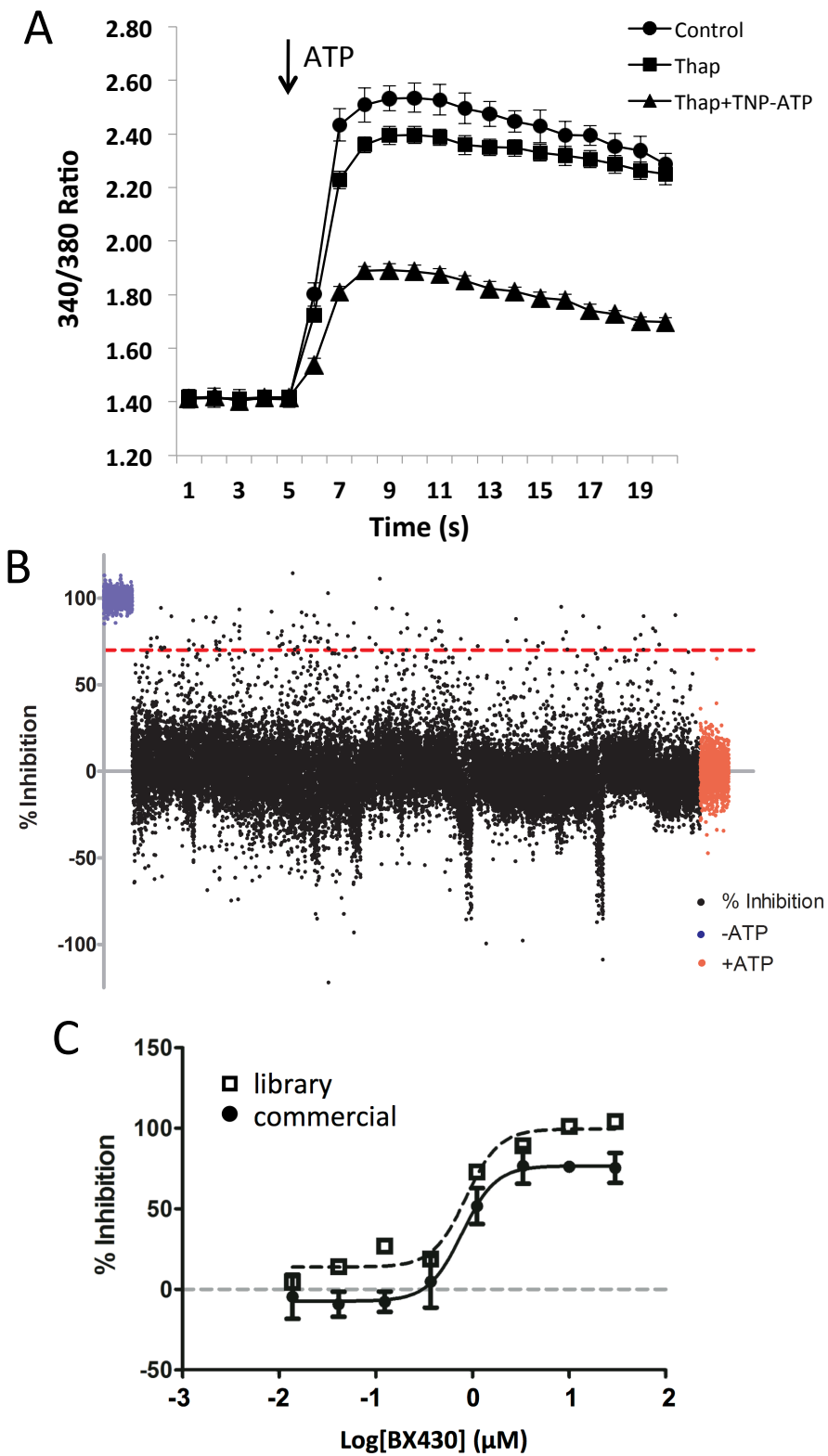
A
ATP
Control
Thap
Thap+TNP-ATP
340/380 Ratio
2.80
2.60
2.40
2.20
2.00
1.80
1.60
1.40
1.20
1
3
5
7
9
11
13
15
17
19
Time (s)
B
% Inhibition
100
50
0
-50
-100
% Inhibition
-ATP
+ATP
C
library
commercial
% Inhibition
150
100
50
0
-50
-3
-2
-1
0
1
2
Log[BX430] (μM)

Figure 2

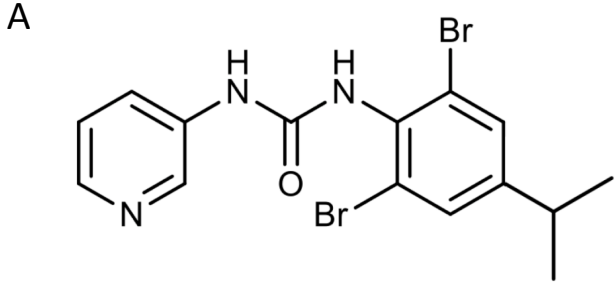
A
H
N
H
N
O
Br
Br
N

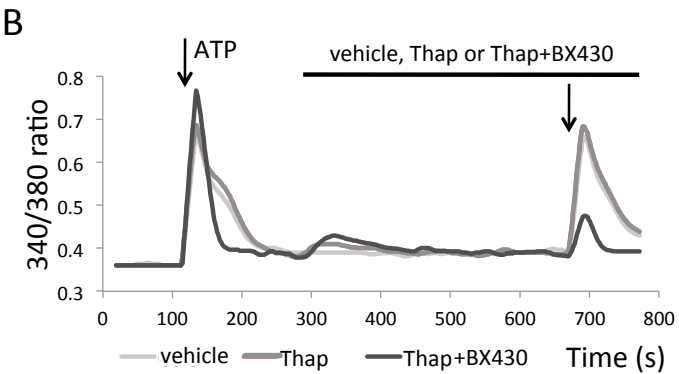
B
ATP
vehicle, Thap or Thap+BX430
340/380 ratio
0.8
0.7
0.6
0.5
0.4
0.3
0
100
200
300
400
500
600
700
800
vehicle
Thap
Thap+BX430
Time (s)

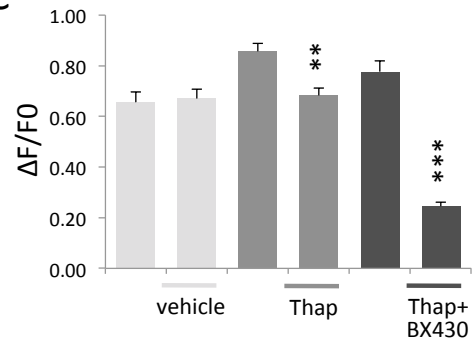
C
ΔF/F0
1.00
0.80
0.60
0.40
0.20
0.00
**
***
vehicle
Thap
Thap+
BX430

Figure 3

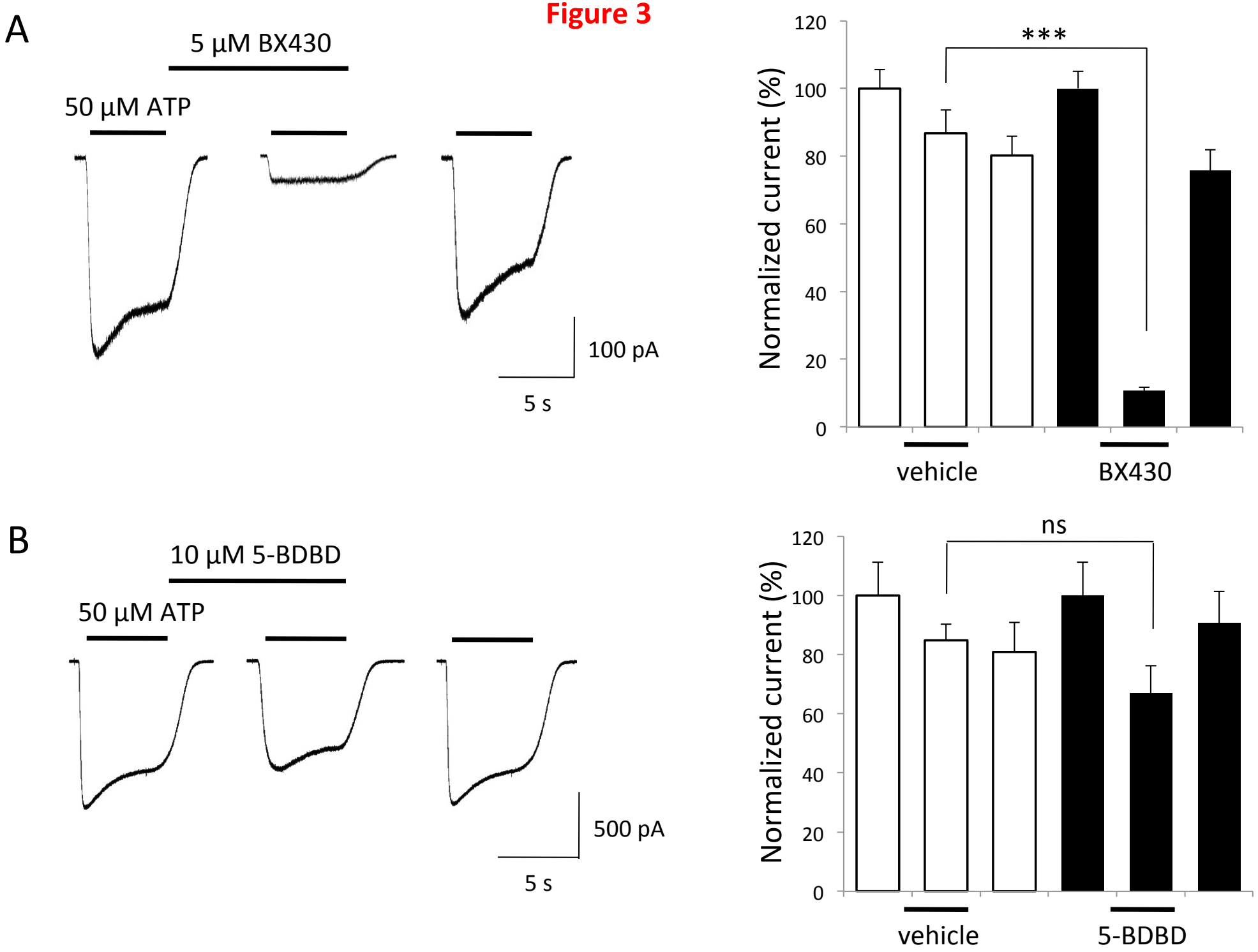
A
5 μM BX430
50 μM ATP
100 pA
5 s
Normalized current (%)
120
100
80
60
40
20
0
***
vehicle
BX430
B
10 μM 5-BDBD
50 μM ATP
500 pA
5 s
Normalized current (%)
120
100
80
60
40
20
0
ns
vehicle
5-BDBD

Figure 4

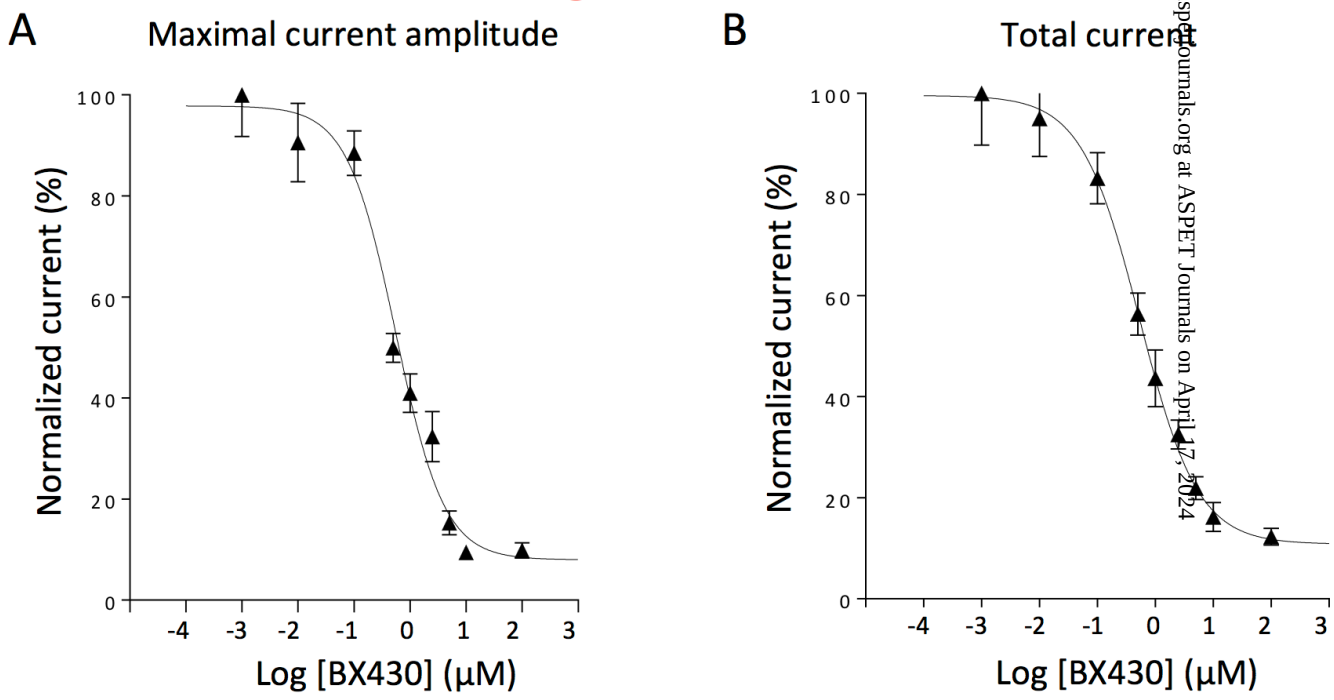

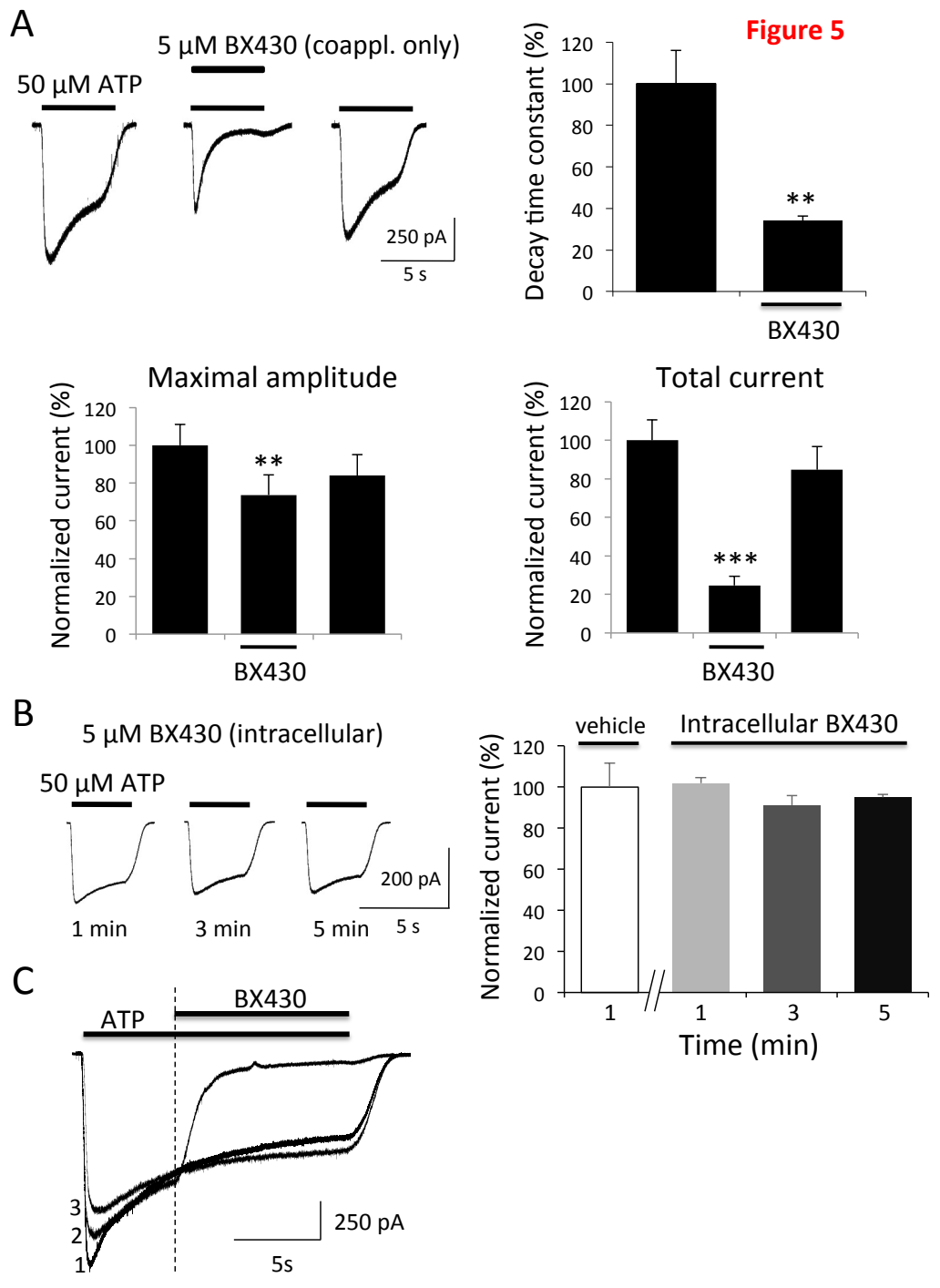
A
5 µM BX430 (coappl. only)
50 µM ATP
250 pA
5 s
Figure 5
Decay time constant (%)
120
100
80
60
40
20
0
**
BX430
Maximal amplitude
Normalized current (%)
120
100
80
60
40
20
0
**
BX430
Total current
Normalized current (%)
120
100
80
60
40
20
0
***
BX430
B
5 µM BX430 (intracellular)
50 µM ATP
200 pA
5 s
1 min
3 min
5 min
vehicle
Intracellular BX430
Normalized current (%)
120
100
80
60
40
20
0
1
1
3
5
Time (min)
C
ATP
BX430
3
2
1
250 pA
5s

Figure 6

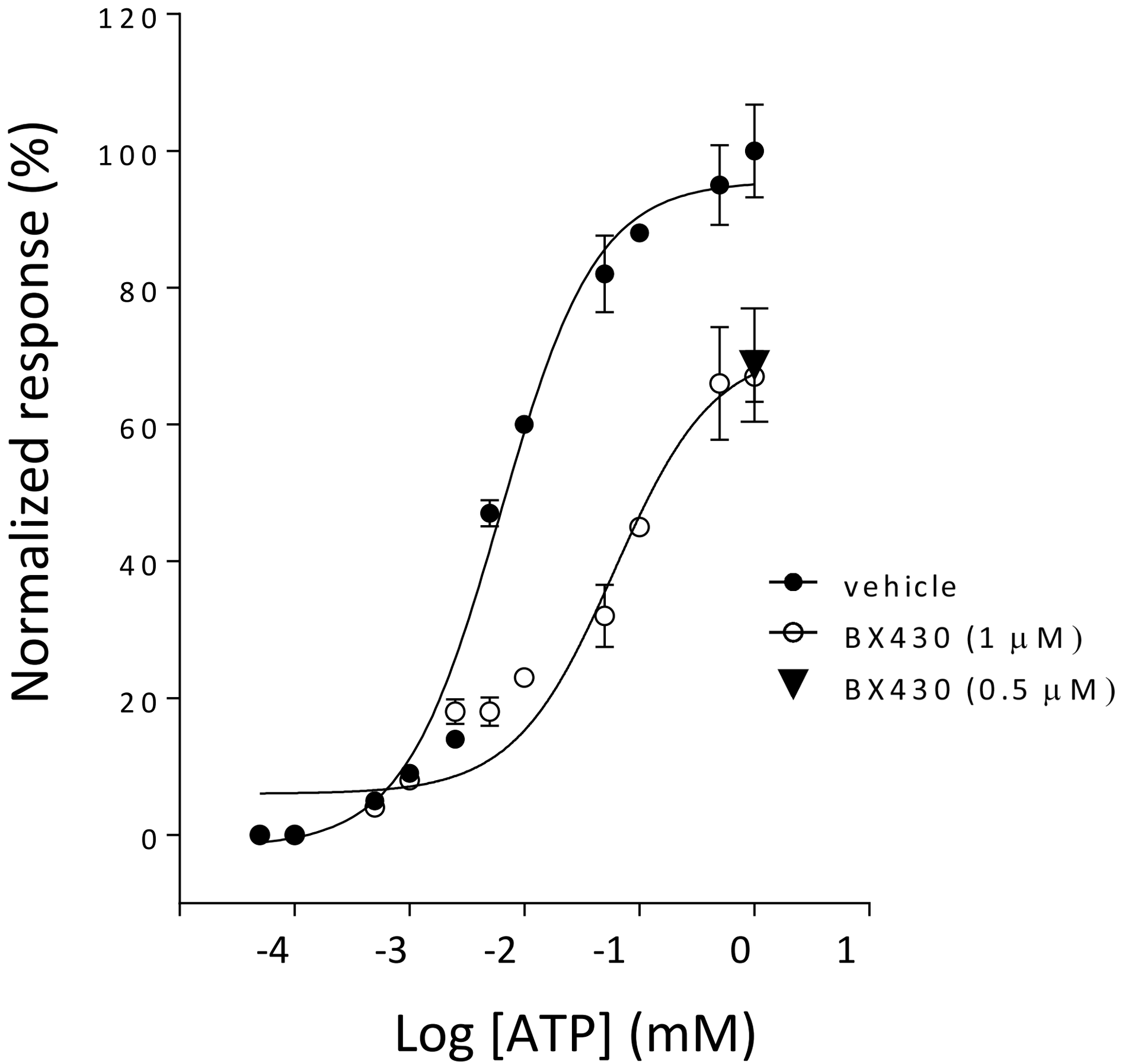
120
100
80
60
40
20
0
Normalized response (%)
-4
-3
-2
-1
0
1
Log [ATP] (mM)
vehicle
BX430 (1 μM)
BX430 (0.5 μM)

Figure 7

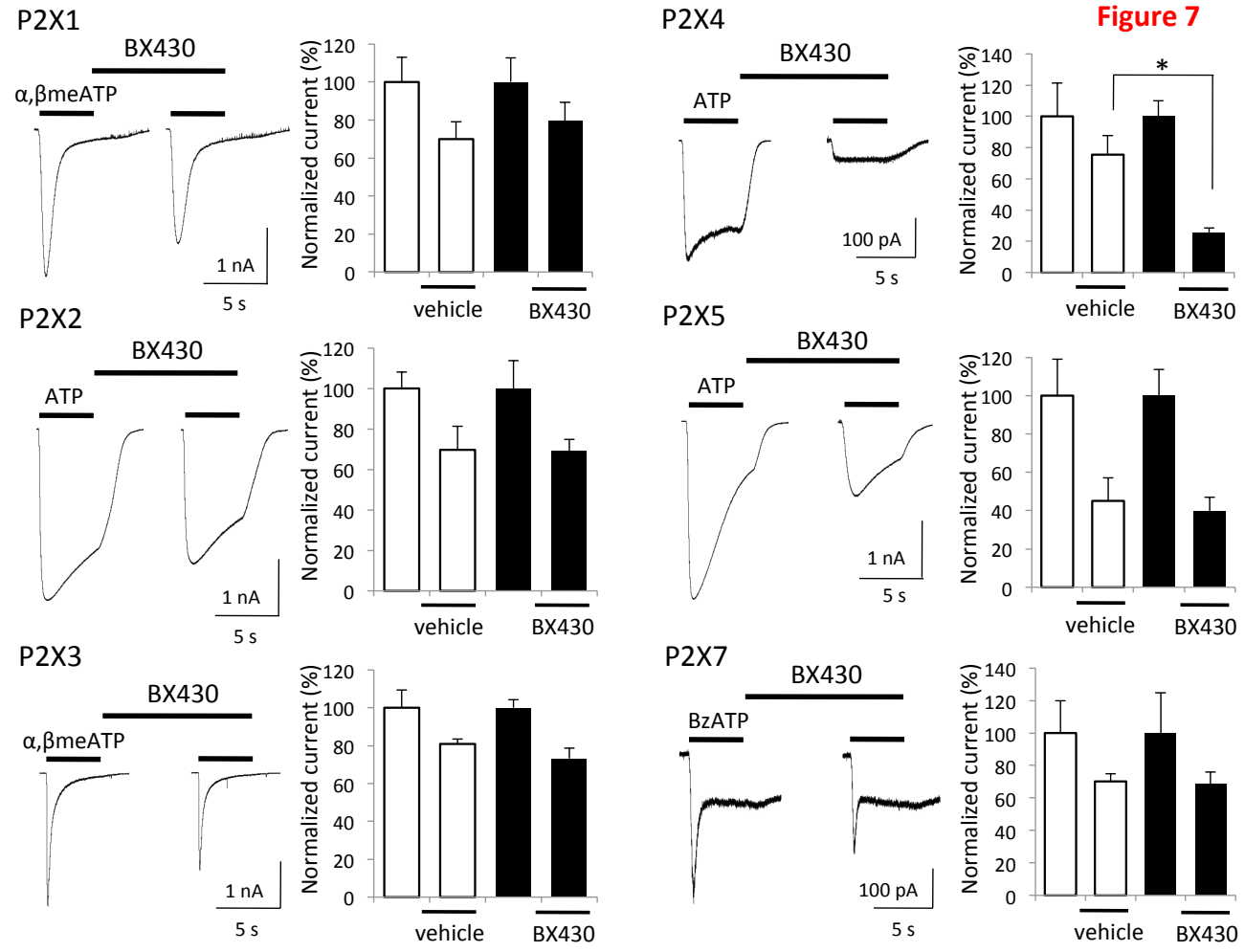
P2X1
BX430
α,βmeATP
1 nA
5 s
Normalized current (%)
vehicle
BX430
P2X4
BX430
ATP
100 pA
5 s
*
P2X2
BX430
ATP
1 nA
5 s
P2X5
BX430
ATP
1 nA
5 s
P2X3
BX430
α,βmeATP
1 nA
5 s
P2X7
BX430
BzATP
100 pA
5 s

Figure 8

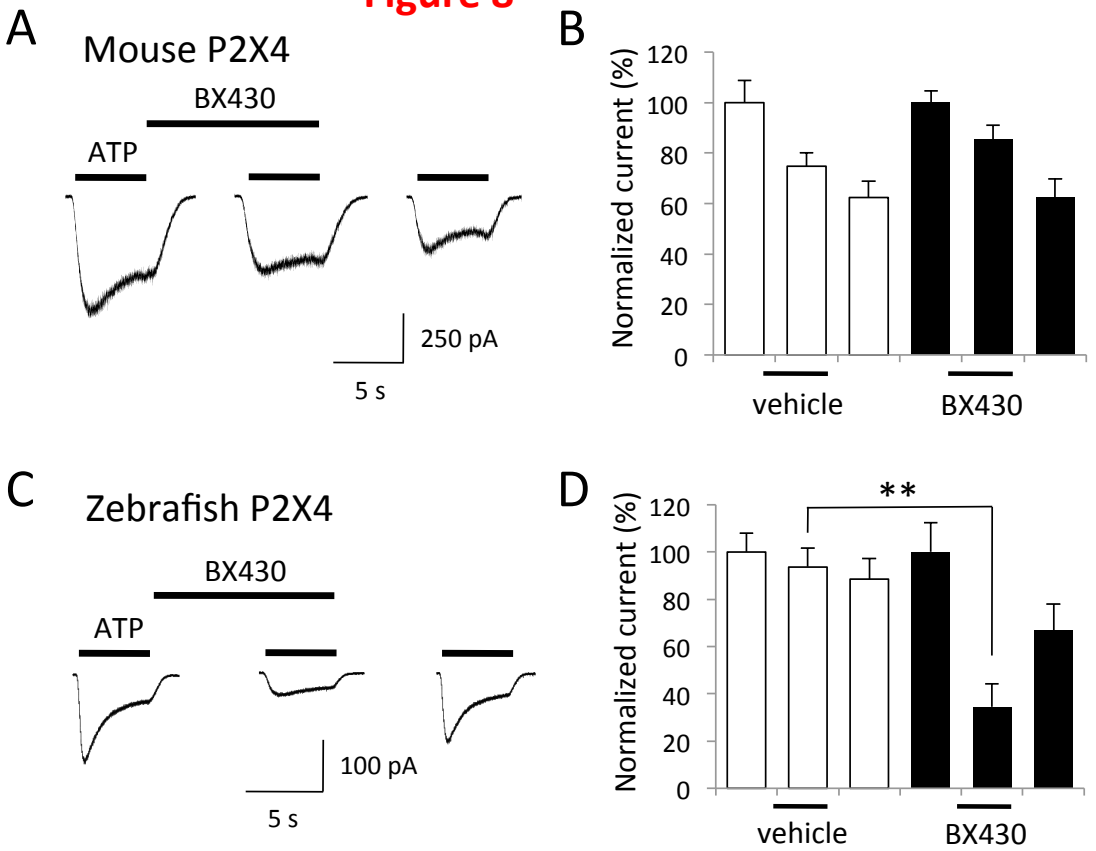
A
Mouse P2X4
BX430
ATP
250 pA
5 s
B
Normalized current (%)
120
100
80
60
40
20
0
vehicle
BX430
C
Zebrafish P2X4
BX430
ATP
100 pA
5 s
D
**
Normalized current (%)
120
100
80
60
40
20
0
vehicle
BX430

A
Figure 9
***
*
Normalized current (%)
350
300
250
200
150
100
50
0
IVM
IVM+BX430
B
IVM
IVM+BX430
Fluorescence (a.u.)
2300
2100
1900
1700
1500
1300
1100
900
700
500
50
100
150
200
250
300
Time (s)

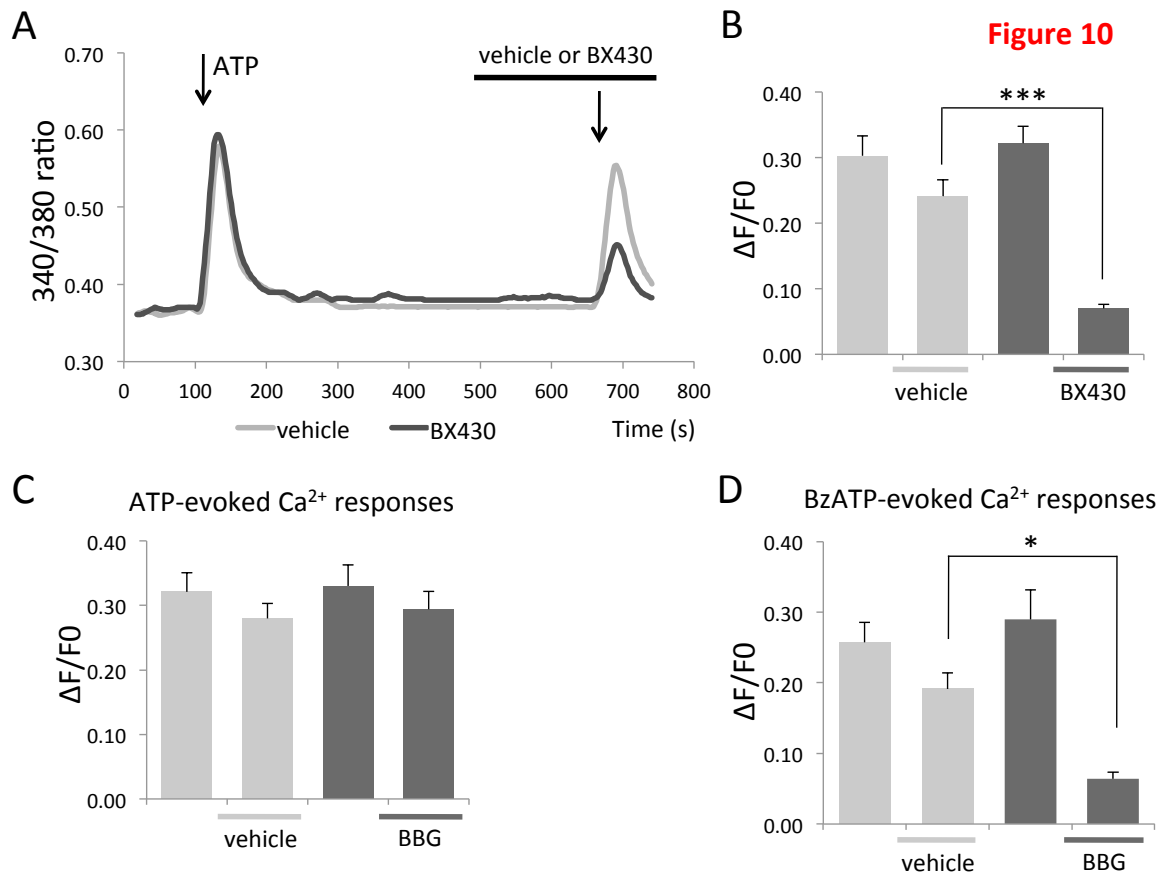
A
ATP
vehicle or BX430
340/380 ratio
0.70
0.60
0.50
0.40
0.30
0
100
200
300
400
500
600
700
800
vehicle
BX430
Time (s)
B
Figure 10
***
ΔF/F0
0.40
0.30
0.20
0.10
0.00
vehicle
BX430
C
ATP-evoked Ca2+ responses
ΔF/F0
0.40
0.30
0.20
0.10
0.00
vehicle
BBG
D
BzATP-evoked Ca2+ responses
*
ΔF/F0
0.40
0.30
0.20
0.10
0.00
vehicle
BBG